Electronic Supplementary Material (ESI) for New Journal of Chemistry.

Magnetically Separable Type-II Semiconductor based ZnO/MoO_3 Photocatalyst: A Proficient System for Heteroarenes Arylation and Rhodamine B Degradation under Visible Light

Bhawna Kaushik[a], Pooja Rana[a], Deepti Rawat[b], Kanika Solanki[a], Sneha Yadav[a], Pooja Rana[a], R.K. Sharma[a]*

[a]Green Chemistry Network Centre, Department of Chemistry, University of Delhi, New Delhi-110007, India; Tel: 011-276666250, E-mail: rksharmagreenchem@hotmail.com

[b] Department of Chemistry, Miranda House College, University of Delhi, New Delhi-110007, India.

Table of Contents

1. Results and discussion

1.1. Spectrum of the Philips LED

The below provide spectrum shows the emission in the range of 400-800 nm.

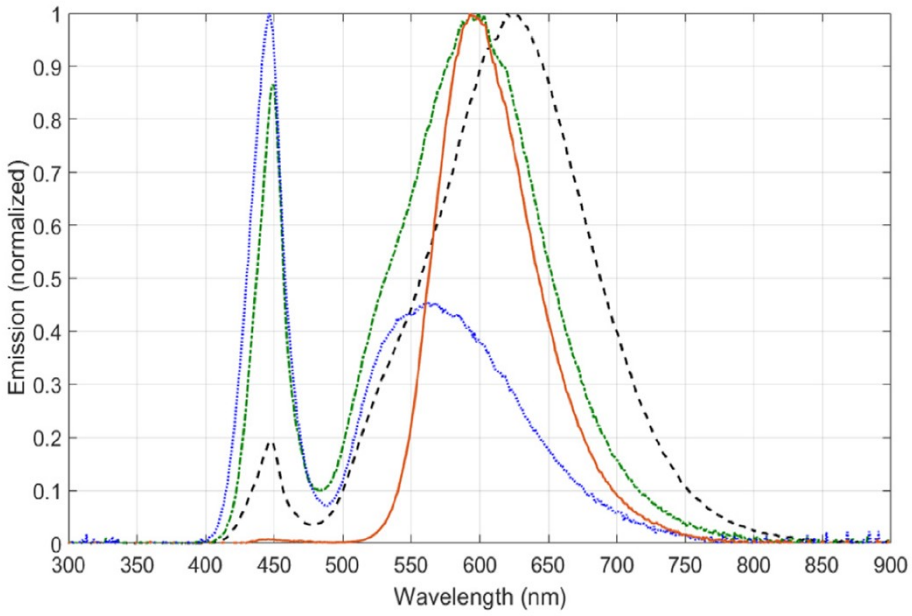

Fig. S1. Normalized spectrum of LED lamps found in street lightings. PC Amber from Philips with CCT of 1765 K (orange solid). Warm from Ignialight with CCT of 2159 K (black dashed). LED from Madrid street lights with CCT of 3107 K (green dash-dot). BLED at Faculty of Pharmacy from Universidad Complutense with CCT of 6801 K (blue dots) [1, 2]. Reproduced with permission from ref. [1] Copyright © 2021 Elsevier B.V.

1.2. SEM Analysis

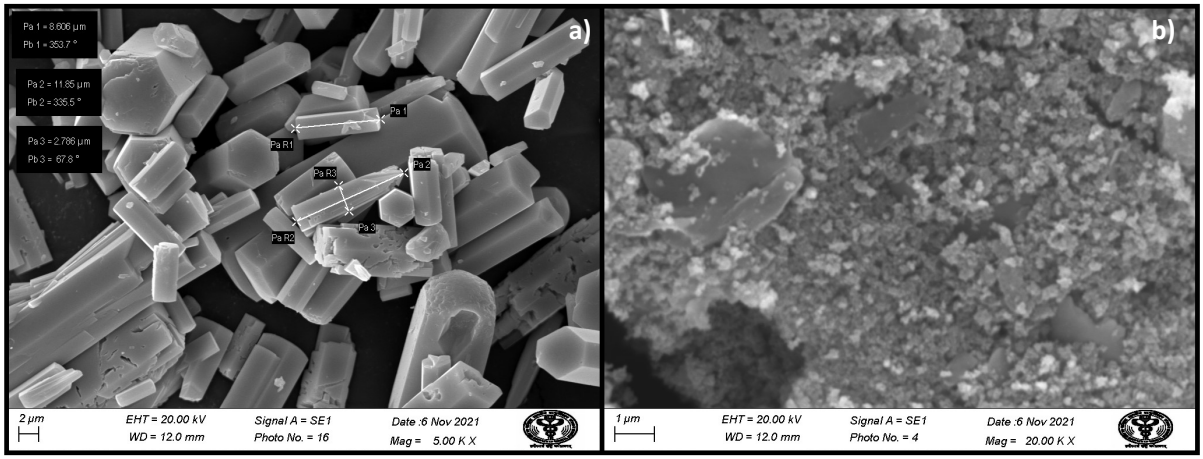

Figure S2. SEM images of a) MoO_3 rods and b) FSZM photocatalyst

1.3. XRD Analysis

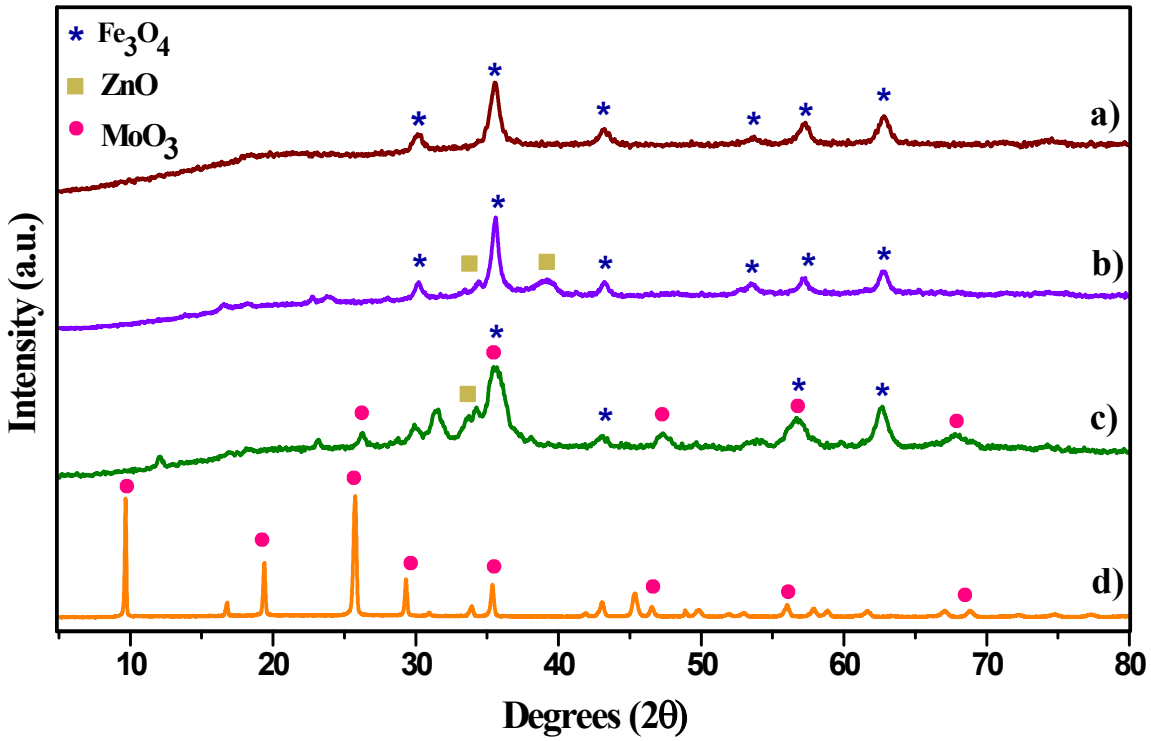

Figure S3. Powder XRD patterns of a) F, b) FSZ, c) FSZM and d) MoO_3 rods.

1.4. FTIR Analysis

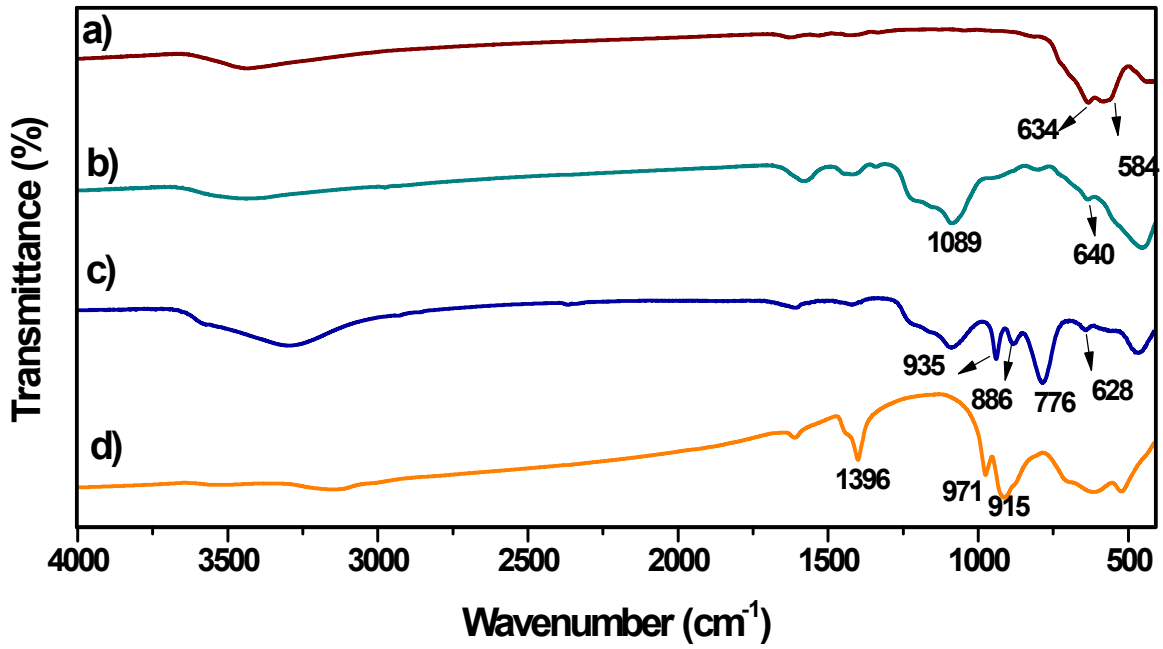

Figure S4. FTIR spectra of a) F, b) FSZ, c) FSZM and d) MoO_3 rods.

1.5. TGA Analysis

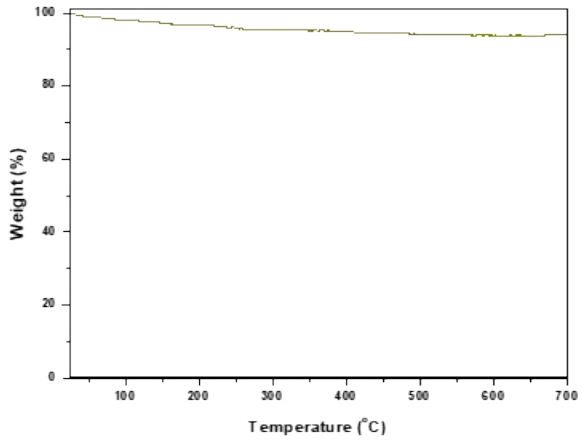

Figure S5. TGA curve of FSZM photocatalyst

1.6. VSM Analysis

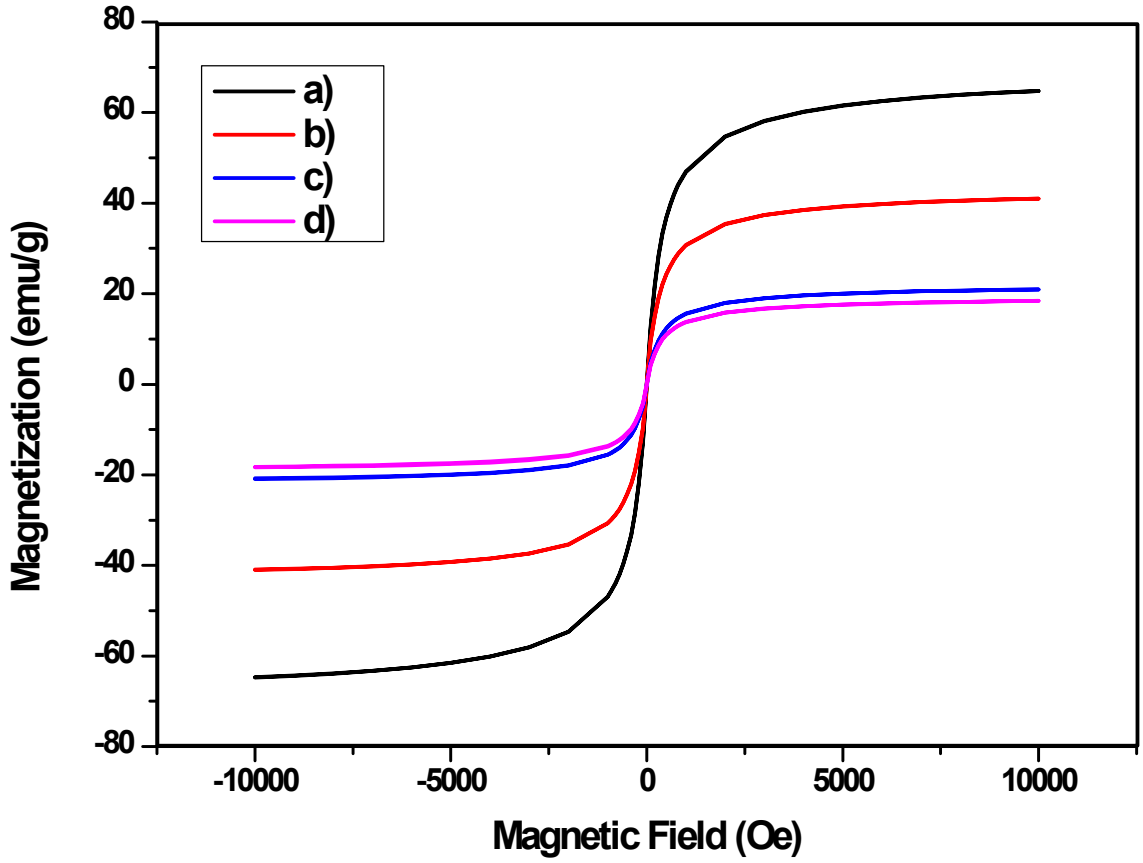

Figure S6. VSM analysis of a) F, b) FS, c) FSZ and d) FSZM photocatalyst

1.7. ED-XRF and EDX Analysis

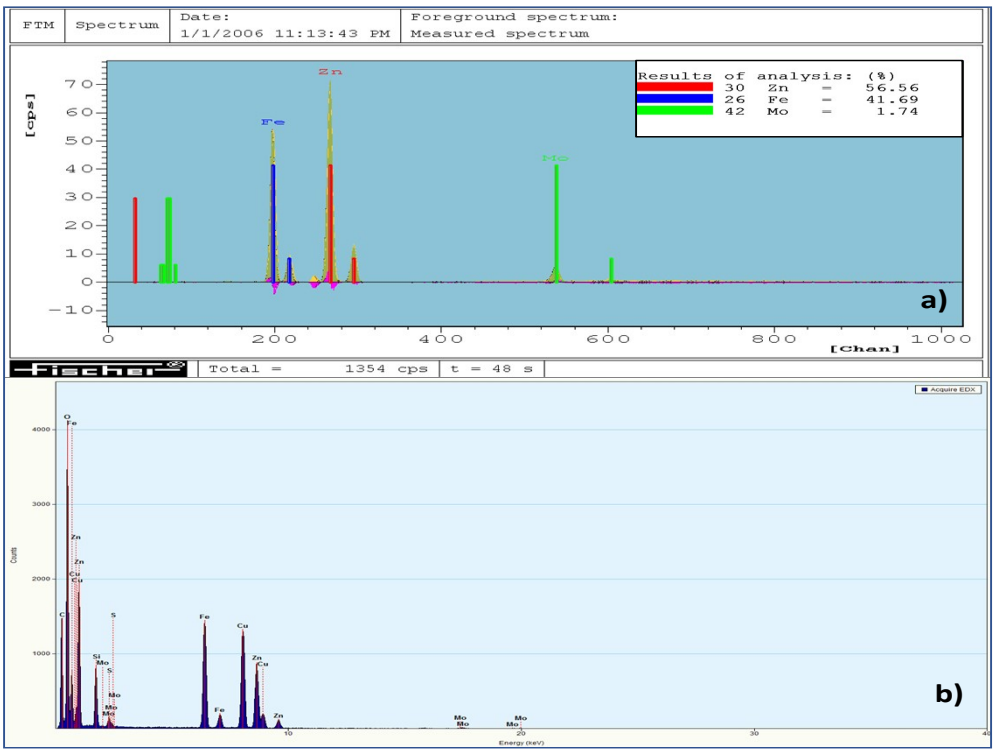

Figure S7. a) EDS and b) ED-XRF spectra of FSZM

2. Tables

Table S1a. Comparison of the catalytic activities of C-H arylation of thiophene with arenes with the earlier reported photocatalysts.

Entry	Catalyst	Light Source	Time	Temp	Reusability	Yield	Ref
1.	Bi_2O_3 (5 mol%)	23 W	15 h	RT	-	47%	[1]
2.	g-C_3N_4/rGO	Daylight lamp	1.5 h	RT	5	74%	[2]
3.	Fe_3O_4@Cu_2xS-MoS_2	Xenon lamp, 300 W	1 h	RT	6	77%	[3]
4.	Black Phosphorous (0.25 mmol)	150 W metal halide lamp	2 h	25 °C	5	75%	[4]
5.	CNPVPy20	White LED lamp, 30 W	1 h	RT	8	83%	[5]
6.	PAF-BT(EDOT)$_2$ (2mg)	23 W energy saving bulb	24 h	RT	5	93%	[6]
7.	(AcrH_2) (10 mol%)	3 W blue LED	12 h	RT	-	73%	[7]
8.	Iodo-bodipys	35 W Xenon lamp	1 h	20 °C	-	72%	[8]
9.	Cercosporin (1 mol%)	Sunlight	16 h	RT	-	69%	[9]
10.	**This work**	**(2×12) W Philips LED bulbs**	**7 h**	**RT**	**5**	**87%**	

Table S1b. Comparison of the degradation efficiency of earlier reported heterogeneous photocatalysts towards Rhodamine B dye

S.No	Catalyst	Oxidants	Dye Concentration	Light source	Time	pH	Degradation percentage	Reusability	Ref
1.	PES/CCTO	-	5 mg/L	360 W UV lamp	40 min	-	74.66 %	-	[10]
2.	TiO_2/ZrO_2	-	10 mg/L	120 W UV light	270 min	7-11	90.5 %	6	[11]
3.	$Bi_xSb_{2-x}S_3$	-	10 mg/L	60 W CFL	30 min	-	98 %	5	[12]
4.	Fe-TiO_2/rGO	8 mM H_2O_2	20 mg/L	150 W Xe lamp	120 min	6	91 %	5	[13]
5.	ZnO	-	10 mg/L	400 W UV lamp	70 min	-	97.7 %	-	[14]
6.	CdS/AgBr-rGO	-	5×10^{-5} M	500 W Xe lamp	60 min	-	95.8 %	4	[15]
7.	Ti-MCM-41	-	1×10^{-4} M	1000 W Xe arc lamp	600 min	-	87 %	-	[16]
9.	Bi_2S_3/3DOM-TiO_2	-	10 mg/L	250 W Xe lamp	360 min	-	96 %	4	[17]
10.	BW/N-B	-	10 mg/L	500 W Xe lamp	45 min	-	99.1 %	4	[18]
11.	ZnO	-	10 mg/L	330 W UV light	160 min	-	95.41 %	-	[19]

12.	SnO_2/ Bi_2S_3-Bi25	-	10 mg/L	300 W sunlight simulated lamp	180 min	-	80.0 %	4	[20]
13.	$FeWO_4$/CNN	-	10 mg/L	Natural sunlight	90 min	-	86.2 %	4	[21]
14.	Au-ZnO	-	10 mg/L	UV light	180 min	6	95 %	-	[22]
15.	TiO_2/g-C_3N_4	-	10 mg/L	500 W xenon lamp	20 min	-	88%	4	[23]
16.	**ZnO/MoO_3**	**-**	**1×10^{-5} M**	**46 W visible light LEDs**	**90 min**	**-**	**96.9 %**	**5**	**Present work**

3. ^{1}H AND ^{13}C NMR data of the corresponding products

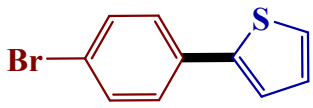

2-(4-bromophenyl) thiophene (3a). The compound was synthesized by adopting General procedure 2.3.1. and purified by column chromatography (100% Petroleum ether). White Solid, Melting Point: 82.4-83.9 °C, ^{1}H-NMR (400 MHz, $CDCl_3$) δ 7.51 (dd, J = 12.5, 8.8 Hz, 4H), 7.33 (d, J = 4.3 Hz, 2H), 7.11 (t, J = 4.4 Hz, 1H); ^{13}C-NMR (101 MHz, $CDCl_3$) δ 143.1, 133.3, 131.9, 128.1, 127.4, 125.2, 123.5, 121.2.

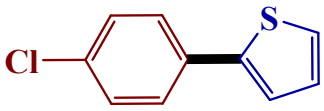

2-(4-chlorophenyl) thiophene (3b). The compound was synthesized by adopting General procedure **A** and purified by column chromatography (100% Petroleum ether). White Solid, Melting Point: 80.0-81.6 °C, ^{1}H-NMR (400 MHz, $CDCl_3$) δ 7.57 (d, J = 8.5 Hz, 2H), 7.37 (d, J = 8.5 Hz, 2H), 7.32 (d, J = 5.0 Hz, 2H), 7.11 (t, J = 4.3 Hz, 1H); ^{13}C-NMR (101 MHz, $CDCl_3$) δ 143.0, 133.2, 132.9, 129.0, 128.1, 127.1, 125.2, 123.4.

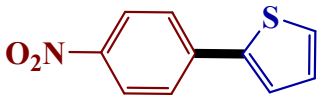

2-(4-nitrophenyl) thiophene (3c). The compound was synthesized by adopting General procedure **A** and purified by column chromatography (100% Petroleum ether). White Solid, Melting Point: 135.2-137.9 °C, ^{1}H-NMR (400 MHz, $CDCl_3$) δ 8.29-8.24 (m, 2H), 7.76 (d, J = 8.8 Hz, 2H), 7.50-7.47 (m, 2H), 7.17 (t, J = 4.3 Hz, 1H); ^{13}C-NMR (101 MHz, $CDCl_3$) δ 146.5, 141.5, 140.5, 128.7, 127.7, 126.0, 125.7, 124.4.

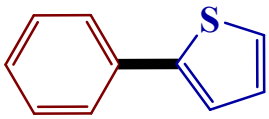

2-phenyl thiophene (3d). The compound was synthesized by adopting General procedure **A** and purified by column chromatography (100% Petroleum ether). Colourless oil, ^{1}H-NMR (400 MHz, $CDCl_3$) δ 7.64 (d, J = 7.5 Hz, 2H), 7.40 (t, J = 7.6 Hz, 2H), 7.34-7.30 (m, 3H), 7.11 (d, J = 8.5 Hz, 1H); ^{13}C-NMR (101 MHz, $CDCl_3$) δ 144.4, 134.4, 128.8, 127.9, 127.4, 125.9, 124.7, 123.0.

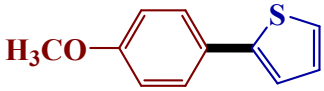

2-(4-methoxyphenyl) thiophene (3e). The compound was synthesized by adopting General procedure **A** and purified by column chromatography (100% Petroleum ether). White Solid, Melting Point: 106.0-108.0 °C, ^{1}H-NMR (400 MHz, $CDCl_3$) δ 7.57 (d, J = 8.8 Hz, 2H), 7.23 (d, J = 9.5 Hz, 2H), 7.09-7.07 (m, 1H), 6.94 (d, J = 8.8 Hz, 2H), 3.86 (s, 3H); ^{13}C-NMR (101 MHz, $CDCl_3$) δ 159.1, 144.3, 127.9, 127.2, 123.8, 122.0, 114.2, 55.3.

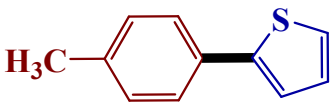

2-(4-methylphenyl) thiophene (3f). The compound was synthesized by adopting General procedure **A** and purified by column chromatography (100% Petroleum ether). Yellow oil, ^{1}H-NMR (400 MHz, $CDCl_3$) δ 7.55 (d, J = 8.3 Hz, 2H), 7.31-7.27 (m, 2H), 7.22 (d, J = 7.8 Hz, 2H), 7.10 (dd, J = 5.0, 3.5 Hz, 1H), 2.40 (s, 3H); ^{13}C-NMR (101 MHz, $CDCl_3$) δ 144.6, 137.3, 129.5, 127.9, 125.9, 124.3, 122.6, 21.2.

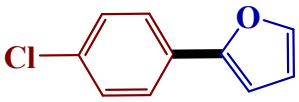

2-(4-chlorophenyl) furan (3g). The compound was synthesized by adopting General procedure **A** and purified by column chromatography (100% Petroleum ether). Colourless Solid, Melting Point: 66-68.2 °C, ^{1}H-NMR (400 MHz, $CDCl_3$) δ 7.59 (dd, J = 6.7, 2.0 Hz, 2H), 7.46 (s, 1H), 7.34 (dd, J = 6.7, 2.1 Hz, 2H), 6.63 (d, J = 3.3 Hz, 1H), 6.47 (q, J = 1.7 Hz, 1H); ^{13}C-NMR (101 MHz, $CDCl_3$) δ 153.0, 142.4, 133.0, 129.4, 128.9, 125.1, 111.8, 105.5.

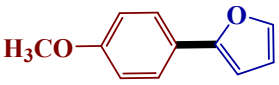

2-(4-methoxyphenyl) furan (3h). The compound was synthesized by adopting General procedure **A** and purified by column chromatography (100% Petroleum ether). White Solid, Melting Point: 48.7-50.0 °C, ^{1}H-NMR (400 MHz, $CDCl_3$) δ 7.59 (d, J = 8.9 Hz, 2H), 7.42 (s, 1H), 6.91 (d, J = 8.9 Hz, 2H), 6.51 (s, 1H), 6.43 (s, 1H), 3.82 (s, 3H); ^{13}C-NMR (101 MHz, $CDCl_3$) δ 159.0, 154.1, 141.4, 125.3, 123.9, 114.1, 111.6, 103.4, 55.4.

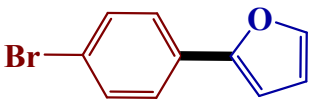

2-(4-bromophenyl) furan (3i). The compound was synthesized by adopting General procedure **A** and purified by column chromatography (100% Petroleum ether). Colourless

Solid, Melting Point: 73.0-74.8 °C, ^{1}H-NMR (400 MHz, $CDCl_3$) δ 7.53-7.46 (m, 5H), 6.64 (s, 1H), 6.47 (s, 1H); ^{13}C-NMR (101 MHz, $CDCl_3$) δ 153.0, 142.4, 131.8, 129.8, 125.3, 121.1, 111.9, 105.6.

4. ^{1}H AND ^{13}C NMR spectra of the corresponding products

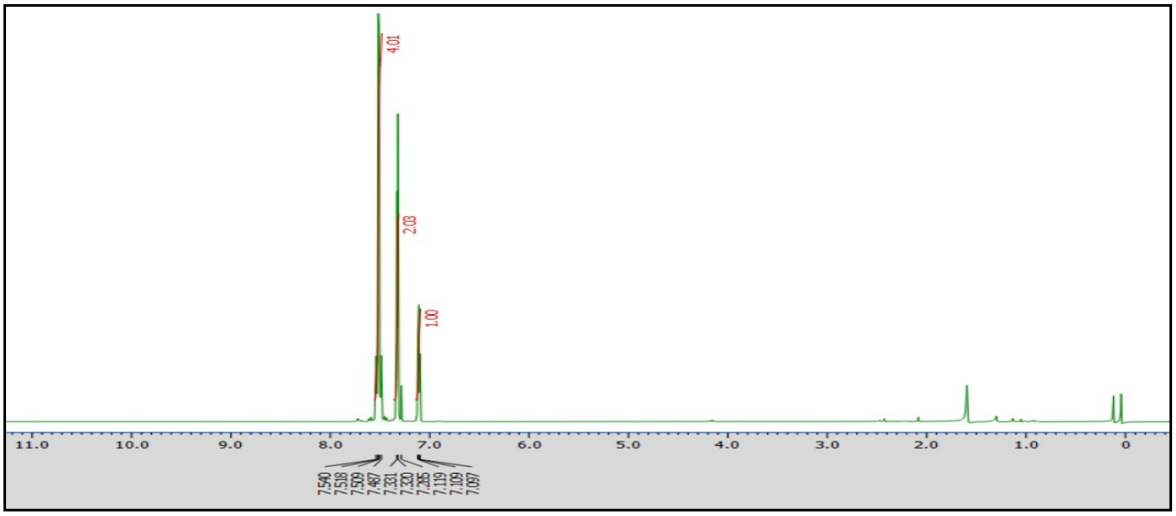

Figure S8. ^{1}H-NMR (400 MHz, $CDCl_3$) of **2-(4-bromophenyl) thiophene** (**3a**).

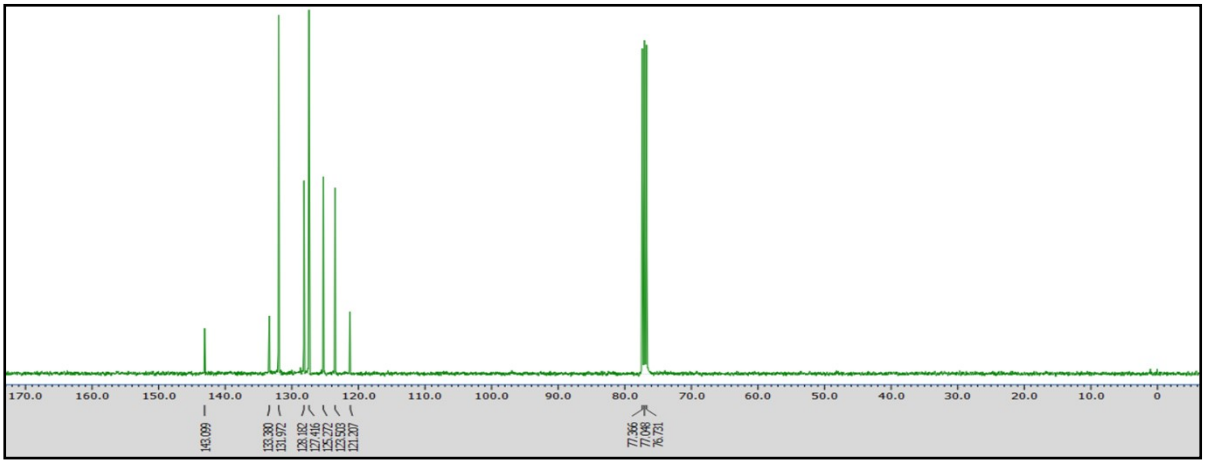

Figure S9. ^{13}C-NMR (101 MHz, $CDCl_3$) of **2-(4-bromophenyl) thiophene** (**3a**).

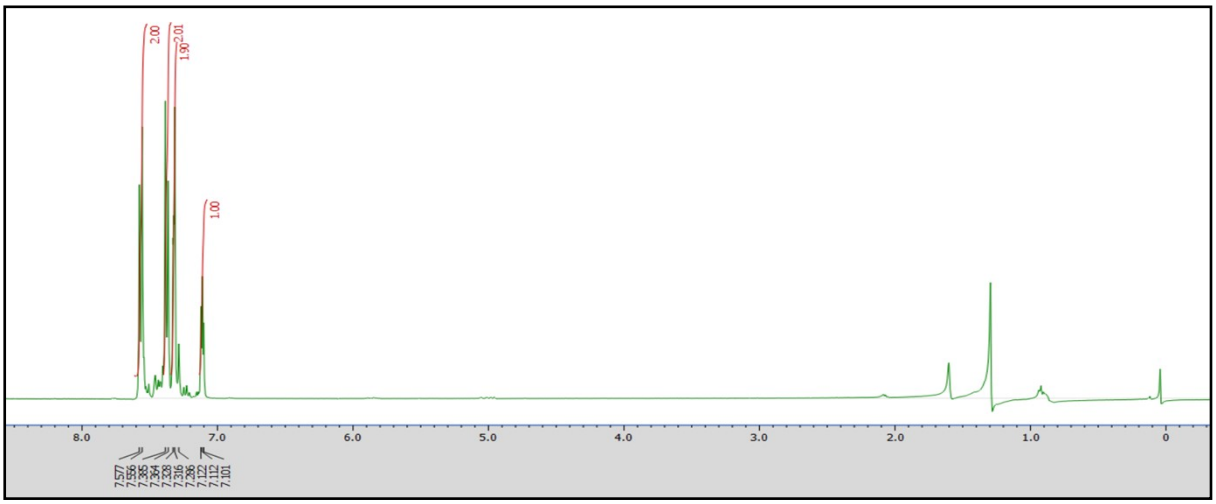

Figure S10. ^{1}H-NMR (400 MHz, $CDCl_3$) of **2-(4-chlorophenyl) thiophene (3b).**

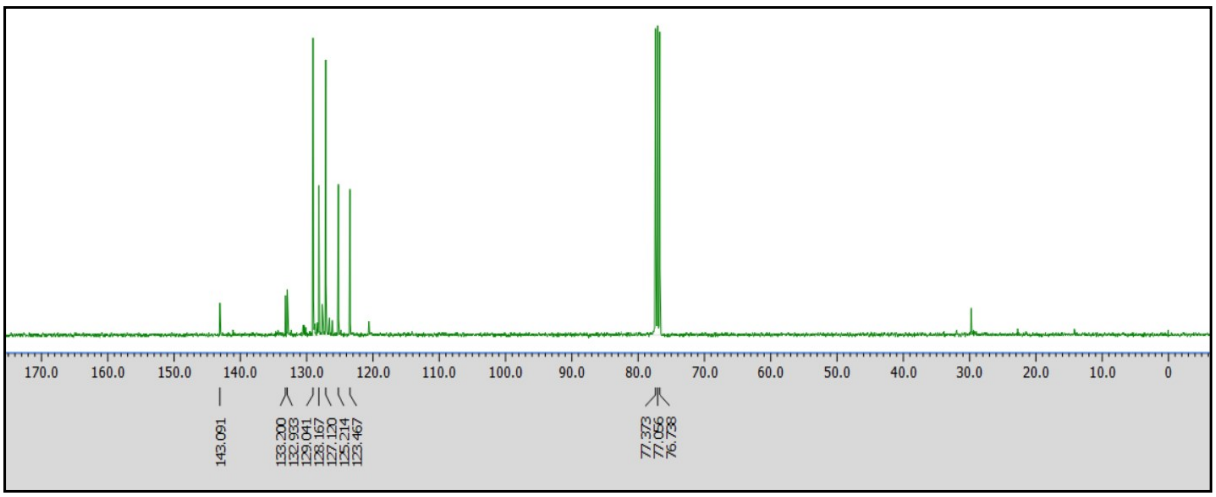

Figure S11. ^{13}C-NMR (101 MHz, $CDCl_3$) of **2-(4-chlorophenyl) thiophene (3b).**

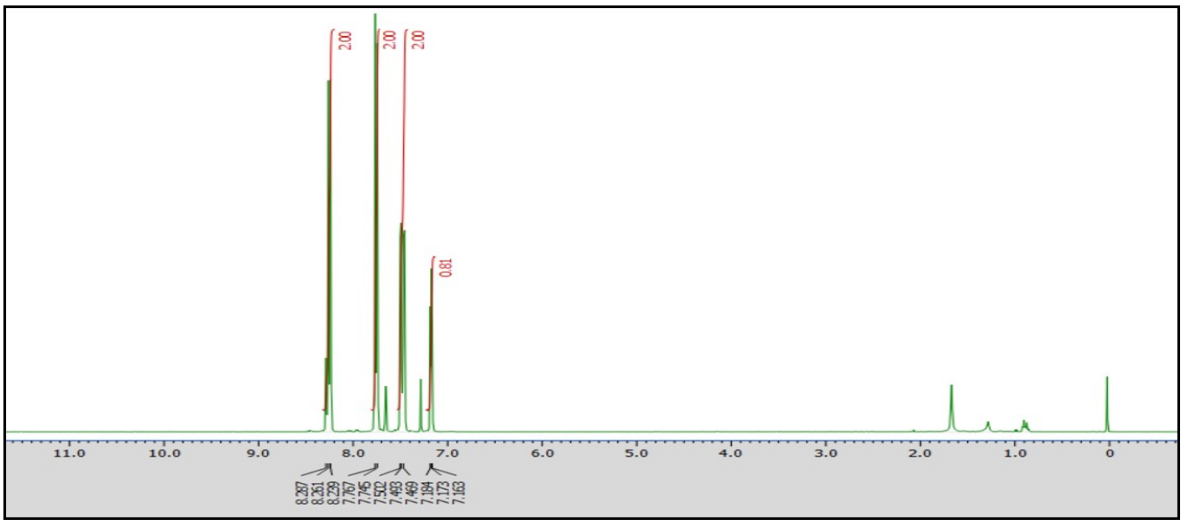

Figure S12. ^{1}H-NMR (400 MHz, $CDCl_3$) of **2-(4-nitrophenyl) thiophene** (**3c**).

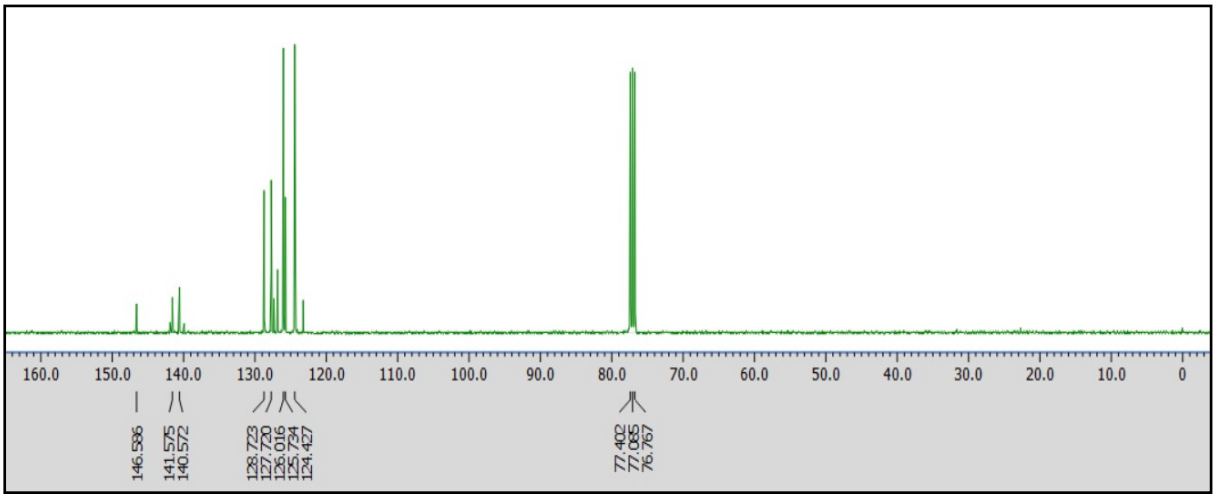

Figure S13. ^{13}C-NMR (101 MHz, $CDCl_3$) of **2-(4-nitrophenyl) thiophene** (**3c**).

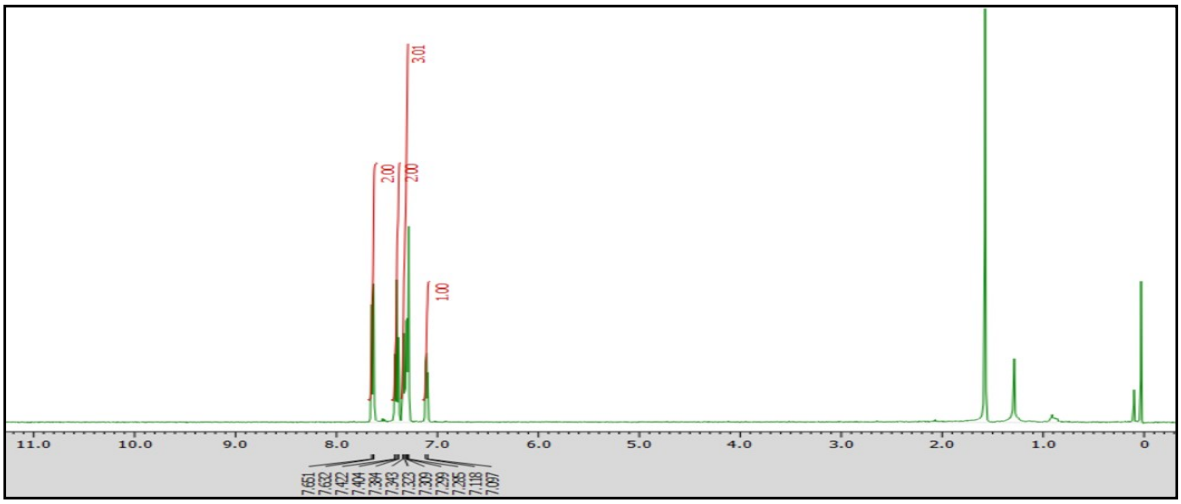

Figure S14. ^{1}H-NMR (400 MHz, $CDCl_3$) of **2-phenyl thiophene** (**3d**).

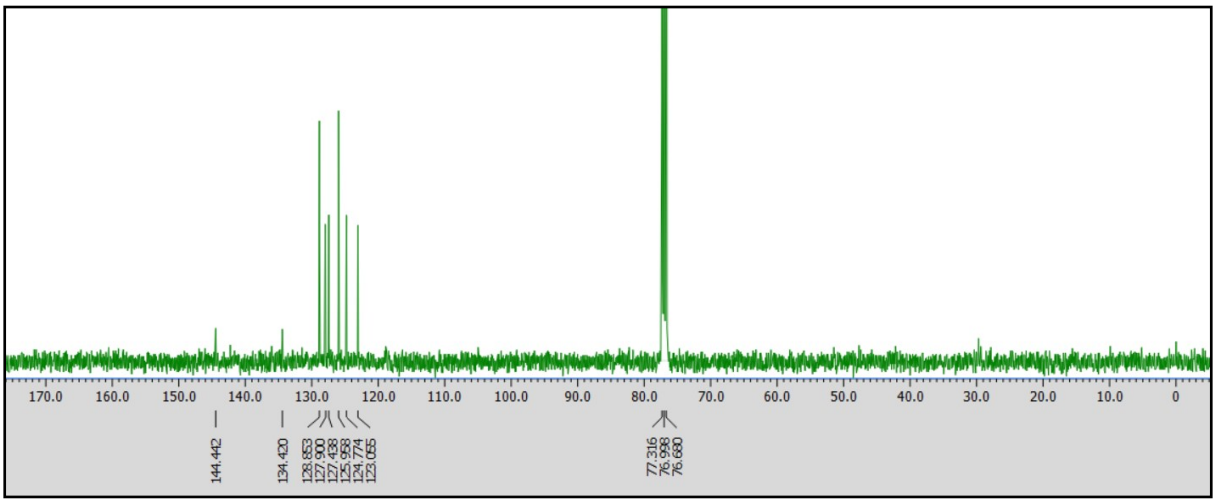

Figure S15. ^{13}C-NMR (101 MHz, $CDCl_3$) of **2-phenyl thiophene** (**3d**).

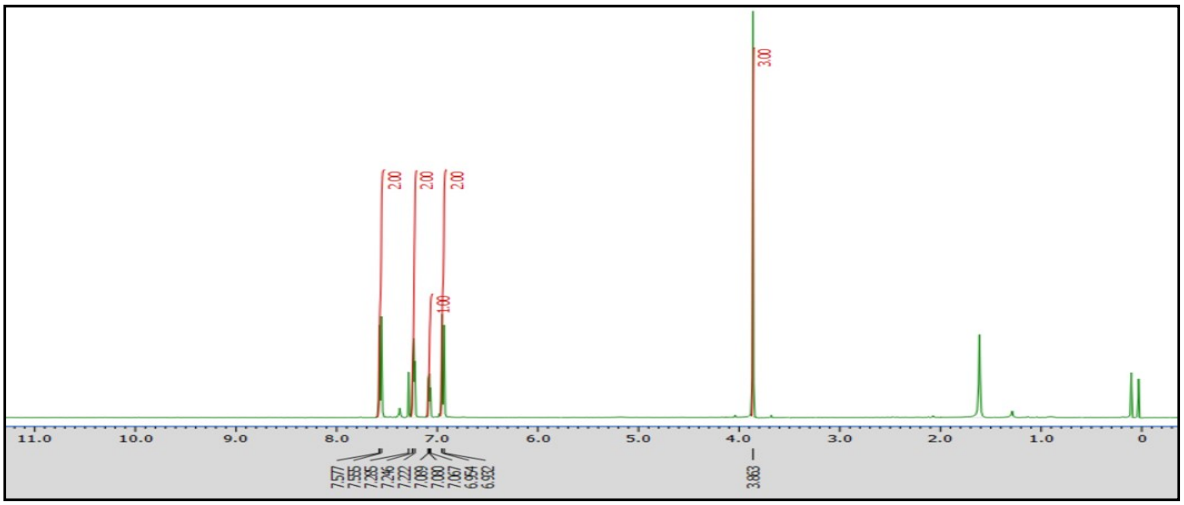

Figure S16. ^{1}H-NMR (400 MHz, $CDCl_3$) of **2-(4-methoxyphenyl) thiophene** (**3e**).

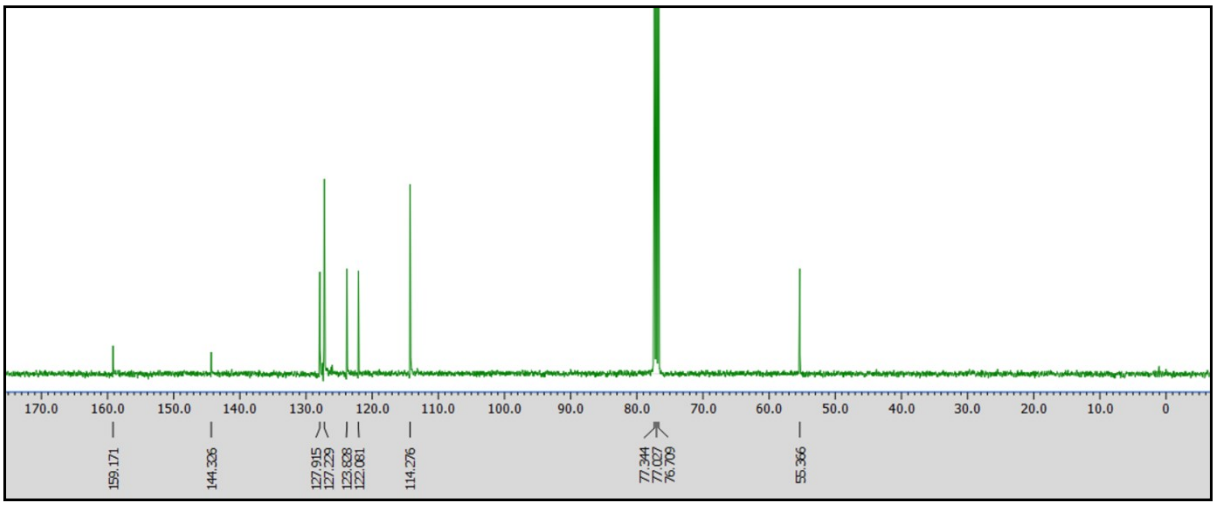

Figure S17. ^{13}C-NMR (101 MHz, $CDCl_3$) of **2-(4-methoxyphenyl) thiophene** (**3e**).

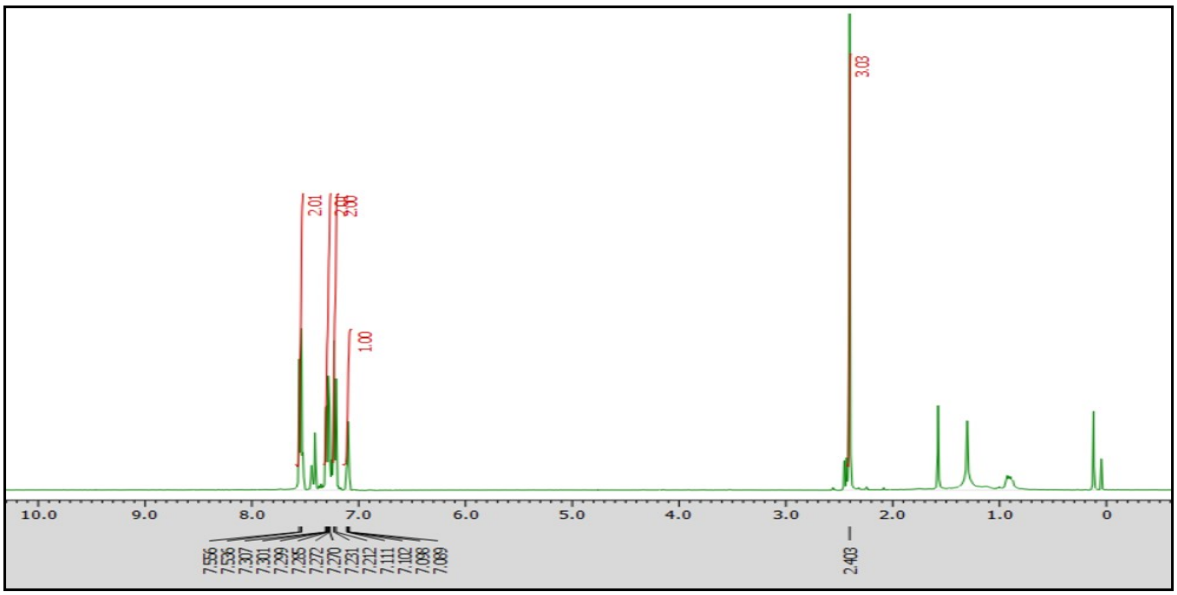

Figure S18. ^{1}H-NMR (400 MHz, $CDCl_3$) of **2-(4-methylphenyl) thiophene** (**3f**).

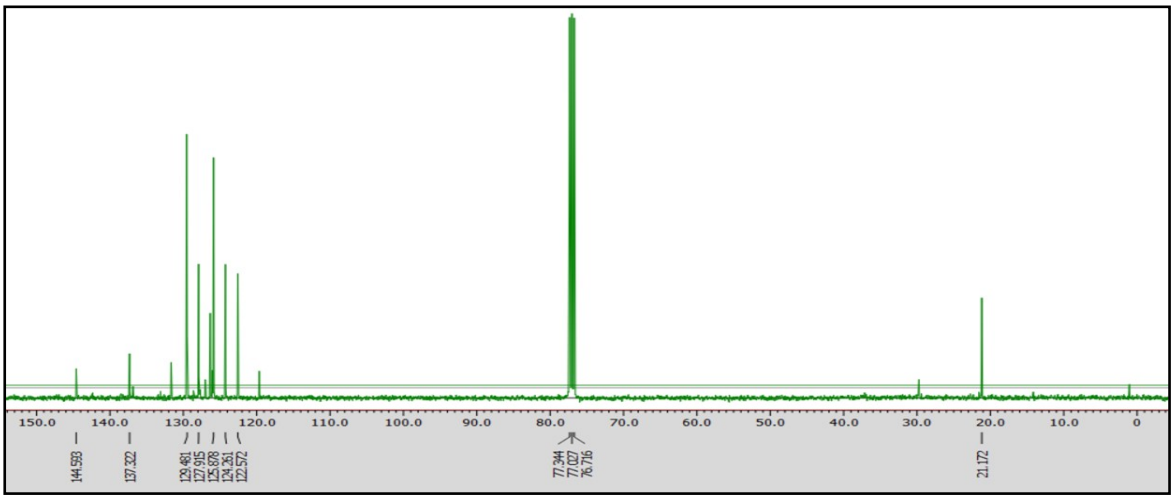

Figure S19. ^{13}C-NMR (101 MHz, $CDCl_3$) of **2-(4-methylphenyl) thiophene** (**3f**).

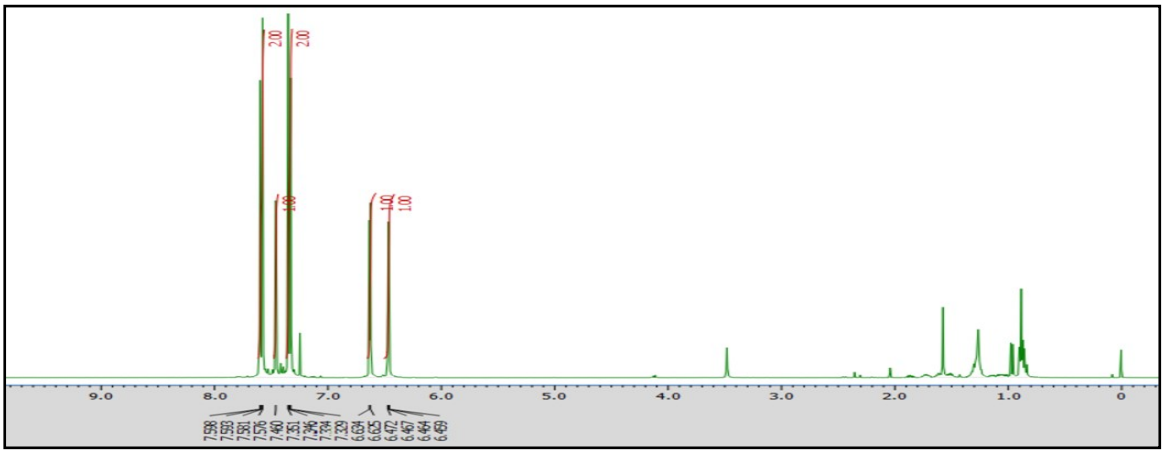

Figure S20. ^{1}H-NMR (400 MHz, $CDCl_3$) of **2-(4-chlorophenyl) furan** (**3g**).

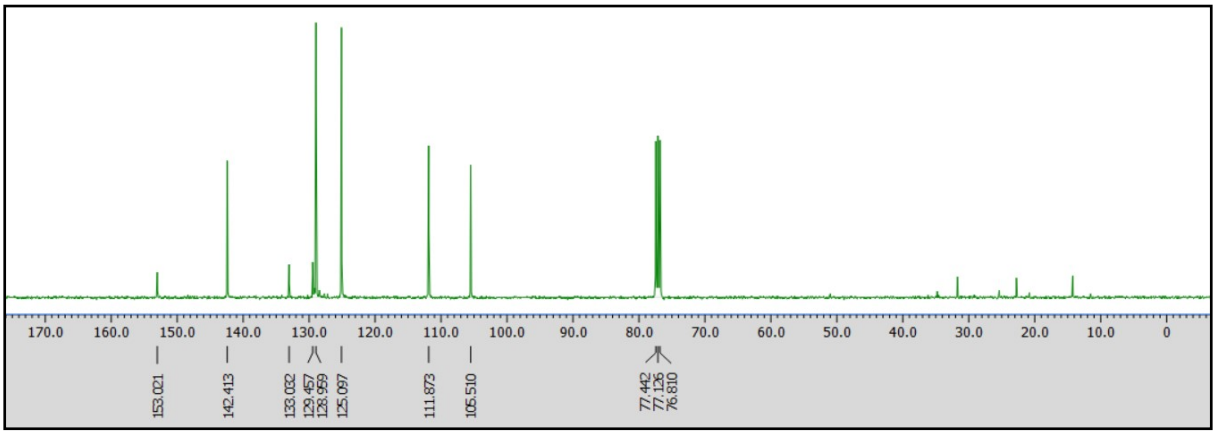

Figure S21. ^{13}C-NMR (101 MHz, $CDCl_3$) of **2-(4-chlorophenyl) furan** (**3g**).

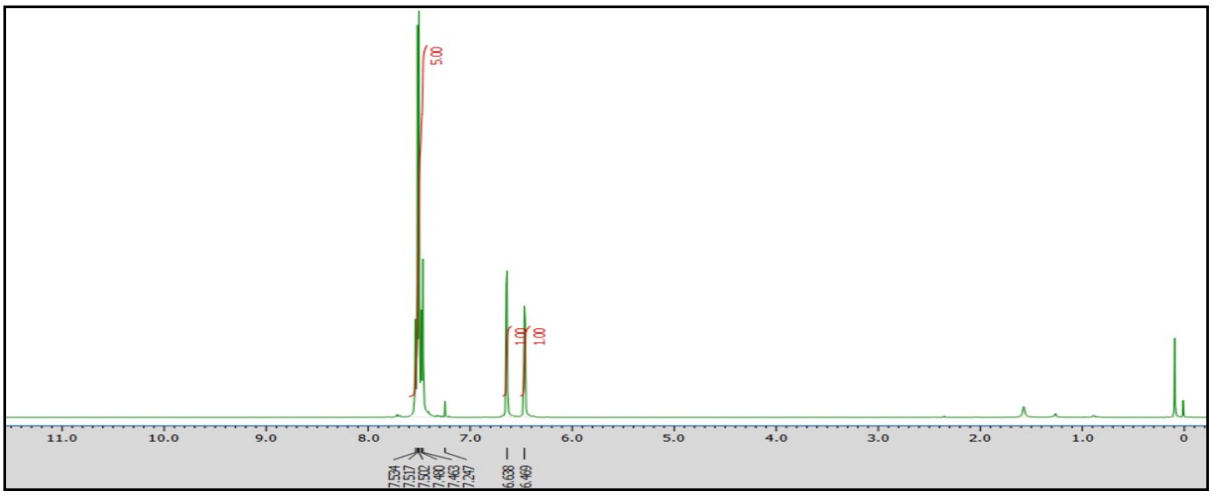

Figure S22. ^{1}H NMR (400 MHz, $CDCl_3$) of **2-(4-bromophenyl) furan (3h)**

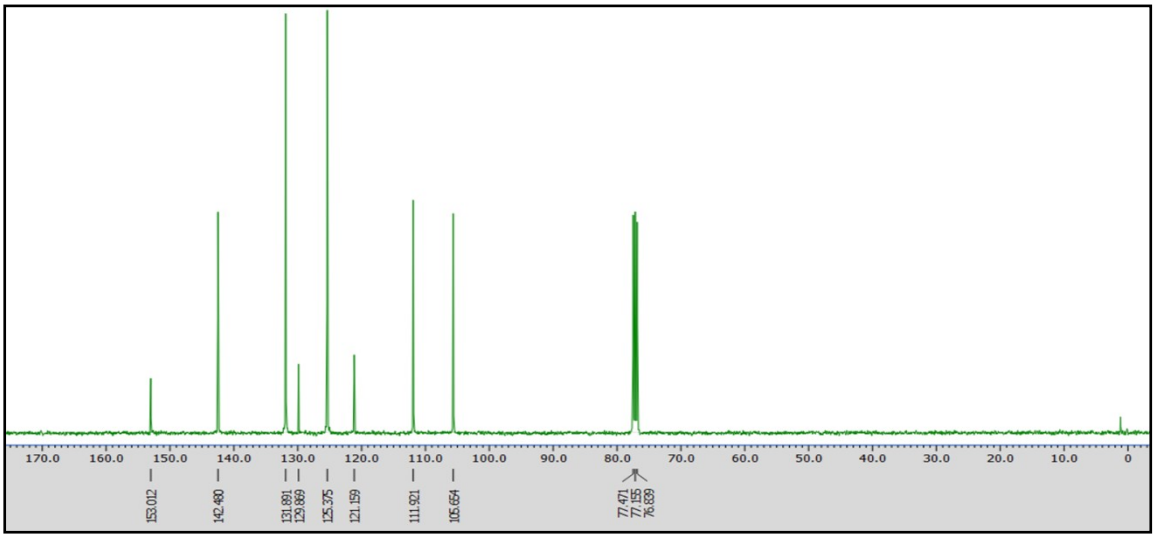

Figure S23. ^{13}C-NMR (400 MHz, $CDCl_3$) of **2-(4-bromophenyl) furan (3h)**

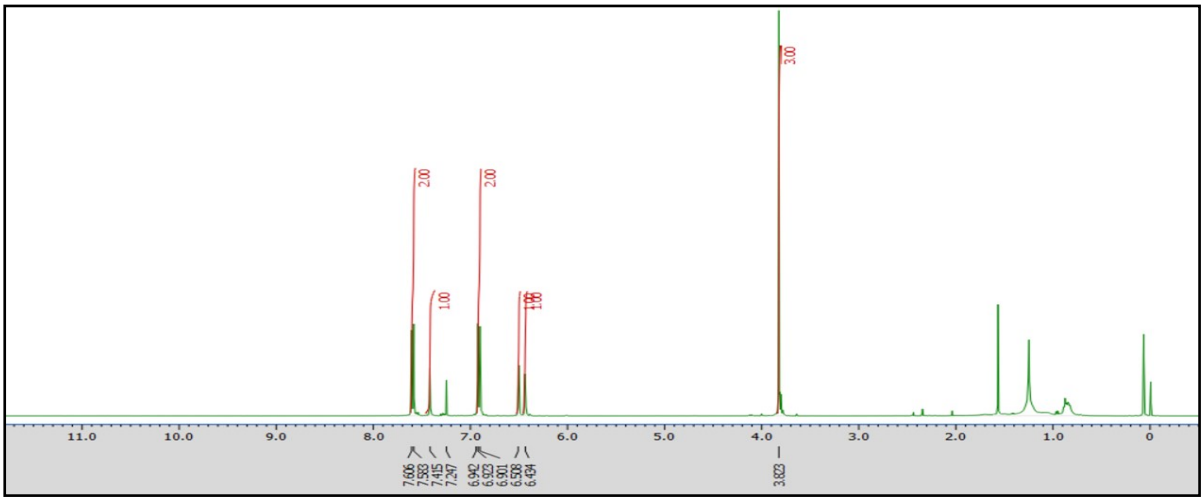

Figure S24. ^{1}H-NMR (400 MHz, $CDCl_3$) of **2-(4-methoxyphenyl) furan** (**3i**).

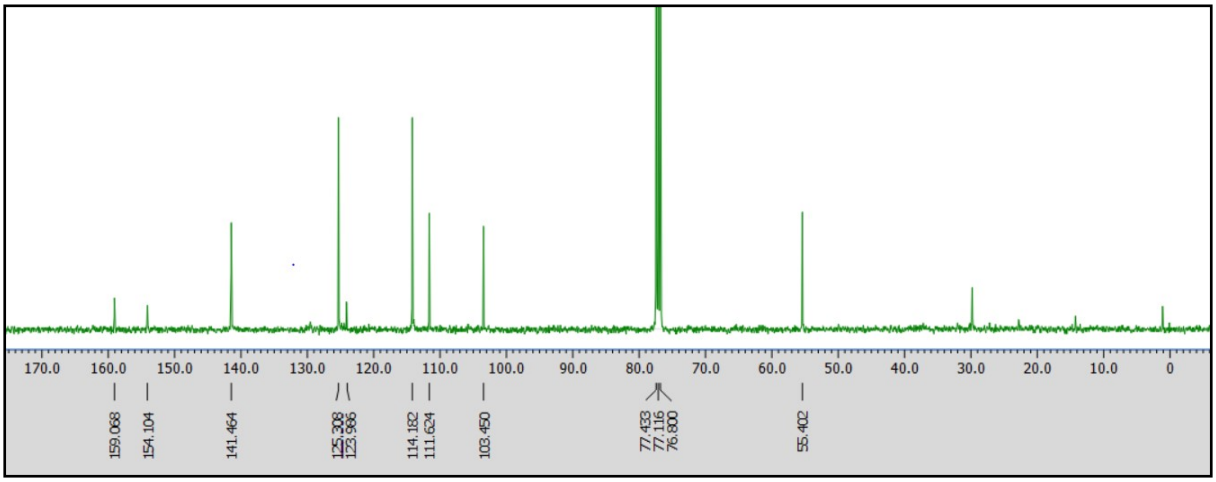

Figure S25. ^{13}C-NMR (101 MHz, $CDCl_3$) of **2-(4-methoxyphenyl) furan** (**3i**).

5. GCMS Spectra

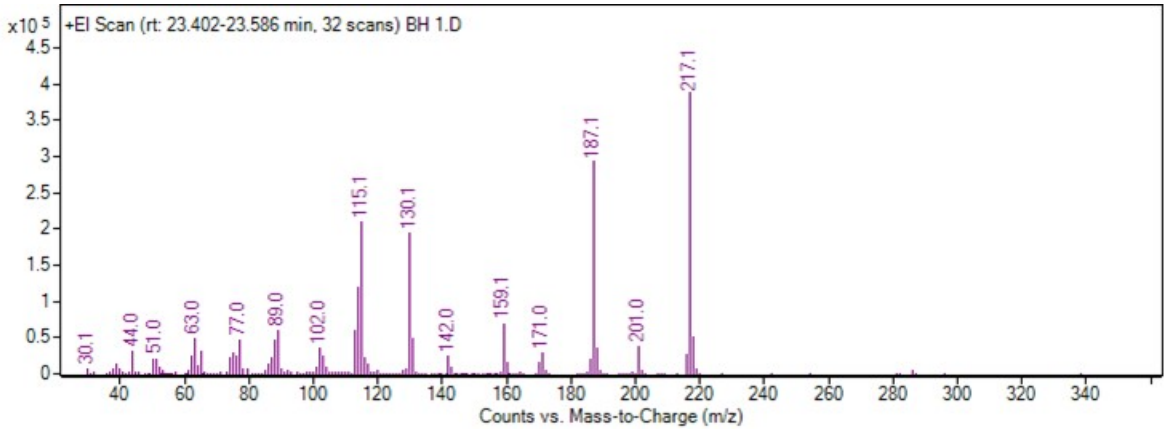

Figure S26. Mass spectra of dantrolene precursor (5-(4-Nitrophenyl)-2-furancarboxaldehyde)

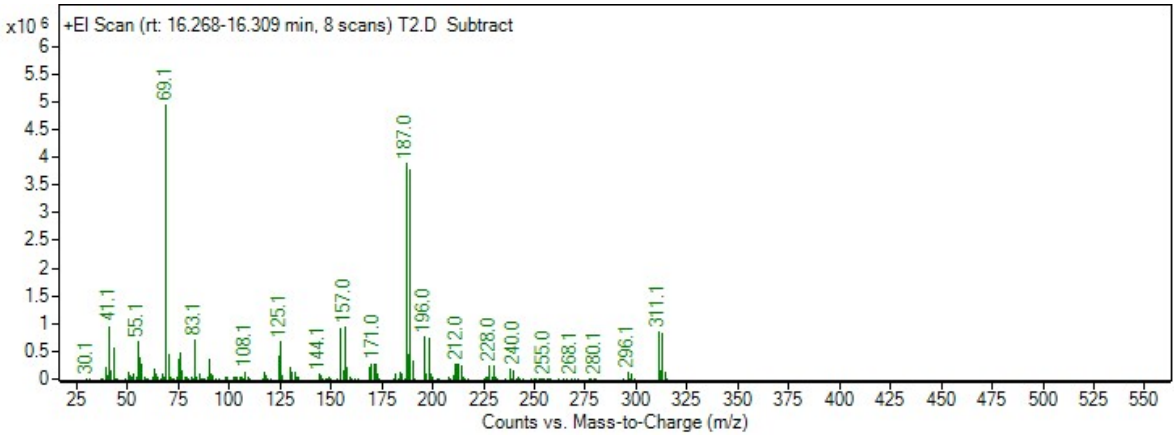

Figure S27. Mass spectra of TEMPO trapped intermediate complex

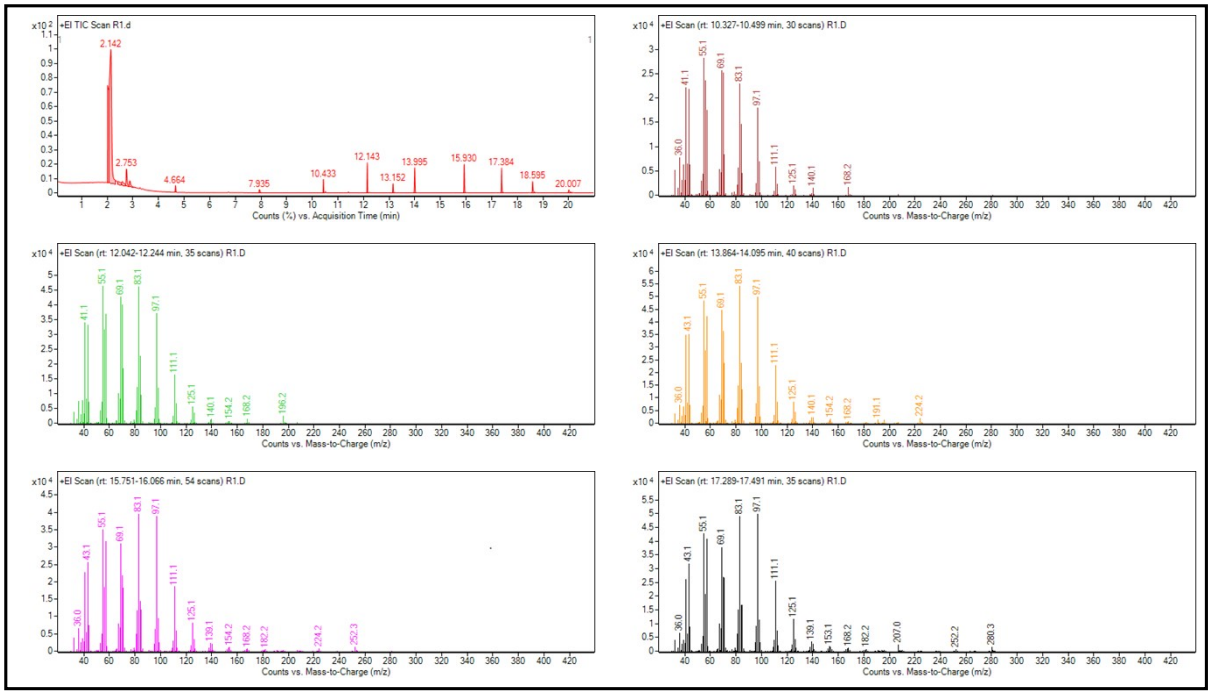

Figure S28. GC-MS spectra of Rhodamine B dye degradation

6. Photoreactor setup

7. References

(1) Buglioni, L.; Riente, P.; Palomares, E.; Pericàs, M. A. Visible-light-promoted arylation reactions photocatalyzed by bismuth (III) oxide. European Journal of Organic Chemistry 2017, 2017 (46), 6986-6990.

(2) Cai, X.; Liu, H.; Zhi, L.; Wen, H.; Yu, A.; Li, L.; Chen, F.; Wang, B. A gC 3 N 4/rGO nanocomposite as a highly efficient metal-free photocatalyst for direct C–H arylation under visible light irradiation. RSC advances 2017, 7 (73), 46132-46138.

(3) Zhi, L.; Zhang, H.; Yang, Z.; Liu, W.; Wang, B. Interface coassembly of mesoporous MoS 2 based-frameworks for enhanced near-infrared light driven photocatalysis. Chemical Communications 2016, 52 (38), 6431-6434.

(4) Kalay, E.; Küçükkeçeci, H.; Kilic, H.; Metin, Ö. Black phosphorus as a metal-free, visible-light-active heterogeneous photoredox catalyst for the direct C–H arylation of heteroarenes. Chemical Communications 2020, 56 (44), 5901-5904.

(5) Liu, J.; Wang, H.; Bai, J.; Li, T.; Yang, Y.; Peng, Y.; Wang, B. Gram-scale synthesis of aligned C 3 N 4–polypyrrole heterojunction aerogels with tunable band structures as efficient visible and near infrared light-driven metal-free photocatalysts. Journal of Materials Chemistry A 2017, 5 (47), 24920-24928.

(6) Huber, N.; Zhang, K. A. Porous aromatic frameworks with precisely controllable conjugation lengths for visible light-driven photocatalytic selective CH activation reactions. European Polymer Journal 2020, 140, 110060.

(7) Feng, Y.-S.; Bu, X.-S.; Huang, B.; Rong, C.; Dai, J.-J.; Xu, J.; Xu, H.-J. NADH coenzyme model compound as photocatalyst for the direct arylation of (hetero) arenes. Tetrahedron Letters 2017, 58 (20), 1939-1942.

(8) Huang, L.; Zhao, J. Iodo-Bodipys as visible-light-absorbing dual-functional photoredox catalysts for preparation of highly functionalized organic compounds by formation of C–C bonds via reductive and oxidative quenching catalytic mechanisms. RSC advances 2013, 3 (45), 23377-23388.

(9) Zhang, S.; Tang, Z.; Bao, W.; Li, J.; Guo, B.; Huang, S.; Zhang, Y.; Rao, Y. Perylenequinonoid-catalyzed photoredox activation for the direct arylation of (het) arenes with sunlight. Organic & biomolecular chemistry 2019, 17 (17), 4364-4369.

(10) Otitoju, T. A.; Jiang, D.; Ouyang, Y.; Elamin, M. A. M.; Li, S. Photocatalytic degradation of Rhodamine B using CaCu3Ti4O12 embedded polyethersulfone hollow fiber membrane. Journal of industrial and engineering chemistry 2020, 83, 145-152.

(11) Tian, J.; Shao, Q.; Zhao, J.; Pan, D.; Dong, M.; Jia, C.; Ding, T.; Wu, T.; Guo, Z. Microwave solvothermal carboxymethyl chitosan templated synthesis of TiO2/ZrO2 composites toward enhanced photocatalytic degradation of Rhodamine B. Journal of colloid and interface science 2019, 541, 18-29.

(12) Dashairya, L.; Mehta, A.; Saha, P.; Basu, S. Visible-light-induced enhanced photocatalytic degradation of Rhodamine-B dye using BixSb2-xS3 solid-solution photocatalysts. Journal of colloid and interface science 2020, 561, 71-82.

(13) Isari, A. A.; Payan, A.; Fattahi, M.; Jorfi, S.; Kakavandi, B. Photocatalytic degradation of rhodamine B and real textile wastewater using Fe-doped TiO2 anchored on reduced graphene oxide (Fe-TiO2/rGO): Characterization and feasibility, mechanism and pathway studies. Applied Surface Science 2018, 462, 549-564.

(14) Nandi, P.; Das, D. Photocatalytic degradation of Rhodamine-B dye by stable ZnO nanostructures with different calcination temperature induced defects. Applied Surface Science 2019, 465, 546-556.

(15) Zhang, J.; Zhang, Z.; Zhu, W.; Meng, X. Boosted photocatalytic degradation of Rhodamine B pollutants with Z-scheme CdS/AgBr-rGO nanocomposite. Applied Surface Science 2020, 502, 144275.

(16) Rasalingam, S.; Peng, R.; Koodali, R. T. An insight into the adsorption and photocatalytic degradation of rhodamine B in periodic mesoporous materials. Applied Catalysis B: Environmental 2015, 174, 49-59.

(17) Ma, G.-q.; Liu, F.-s.; Wang, S.; Dang, Z.-c.; Zhang, J.-w.; Fu, X.-j.; Hou, M.-s. Preparation and characterization of Bi2S3/3DOM-TiO2 for efficient photocatalytic degradation of rhodamine B. Materials Science in Semiconductor Processing 2019, 100, 61-72.

(18) Wang, T.; Liu, S.; Mao, W.; Bai, Y.; Chiang, K.; Shah, K.; Paz-Ferreiro, J. Novel Bi2WO6 loaded N-biochar composites with enhanced photocatalytic degradation of rhodamine B and Cr (VI). Journal of Hazardous materials 2020, 389, 121827.

(19) Dodoo-Arhin, D.; Asiedu, T.; Agyei-Tuffour, B.; Nyankson, E.; Obada, D.; Mwabora, J. Photocatalytic degradation of Rhodamine dyes using zinc oxide nanoparticles. Materials Today: Proceedings 2021, 38, 809-815.

(20) Fenelon, E.; Bui, D.-P.; Tran, H. H.; You, S.-J.; Wang, Y.-F.; Cao, T. M.; Van Pham, V. Straightforward synthesis of SnO2/Bi2S3/BiOCl–Bi24O31Cl10 Composites for drastically enhancing rhodamine B photocatalytic degradation under visible light. ACS omega 2020, 5 (32), 20438-20449.

(21) Dadigala, R.; Bandi, R.; Gangapuram, B. R.; Guttena, V. Construction of in situ self-assembled FeWO 4/gC 3 N 4 nanosheet heterostructured Z-scheme photocatalysts for enhanced photocatalytic